Geometrical Frustration in Nanowire Growth

K. W. Schwarz, J. Tersoff, S. Kodambaka, Y.-C. Chou, and F. M. Ross

Phys. Rev. Lett. **107**, 265502 — Published 23 December 2011

DOI: 10.1103/PhysRevLett.107.265502

Geometrical frustration in nanowire growth

K. W. Schwarz[1], J. Tersoff[1,*], S. Kodambaka[2], Y.-C. Chou[3], and F. M. Ross[1]

[1]*IBM Thomas J. Watson Research Center, Yorktown Heights, New York 10598, USA*

[2]*Department of Materials Science and Engineering, University of California Los Angeles, Los Angeles, California 90095, USA*

[3]*School of Materials Engineering and Birck Nanotechnology Center, Purdue University, West Lafayette, IN 47907, USA*

Idealized nanowire geometries assume stable sidewalls at right angles to the growth front. Here we report growth simulations that include a mix of non-orthogonal facet orientations, as for Au-catalyzed Si. We compare these with *in-situ* microscopy observations, finding striking correspondences. In both experiments and simulations, there are distinct growth modes that accommodate the lack of right angles in different ways – one through sawtooth-textured sidewalls, the other through a growth front at an angle to the growth axis. Small changes in conditions can reversibly switch the growth between modes. The fundamental differences between these modes have important implications for control of nanowire growth.

The vapor-liquid-solid (VLS) process for nanowire growth combines broad technological promise with a captivating elegance. Classic images show slender right prisms of Si growing in the ⟨111⟩ direction, each neatly capped by a droplet of the Au-Si liquid eutectic catalyst from which it grows [1]. Yet this system is perversely complex, and the images are misleading. At high resolution, the Si nanowire sidewalls have been seen to exhibit a surprising sawtooth texture [2,3]. Si nanowires are also observed to grow in ⟨110⟩ and ⟨211⟩ directions [1,4,5,6]. These growth modes exhibit a structure that is different, but again counterintuitive, in that the {111}-faceted liquid-solid interface is now tilted at an angle to the growth direction [1,4,5,7]. The growth direction can be controlled experimentally by the growth conditions [5,8]. This is understood only qualitatively – the surface incorporates Au and/or H or other vapor-derived species, depending on temperature and source-gas pressure, and these in turn affect facet energies [6,8,9,10]. Under some conditions, however, all three modes occur even in wires of similar diameter growing side by side [4,11].

Here we show that such complex behavior arises naturally because this system is geometrically frustrated. For Si, the liquid-solid interface is a (111) facet, but there are apparently no stable facets parallel to ⟨111⟩ for the sidewalls [9,12,13]. To have only stable facets, the wire must grow in some more complicated morphology consistent with the available facet orientations. In the absence of an obvious simple "best" geometry, there may be multiple geometries that are very different but nearly equally favorable, and small changes in the growth conditions can tip the balance between them. We believe that such geometrical frustration is common in diamond and zincblende structure semiconductors, because of the dominant role of the {111} facets.

To address these issues within a simple two-dimensional (2D) model, we consider the crystal structure illustrated in Fig. 1(a,b). Like Si, this has inequivalent sets of facets that allow frustration to be accommodated in different ways. Nanowire growth is then simulated using a well-tested model [10,14]. We find numerous points of agreement between these simulations and our *in situ* experimental observations of nanowire growth, providing compelling evidence that the rich experimental behavior indeed arises largely from geometrical frustration.

Si nanowires were observed during growth in a UHV transmission electron microscope by exposing an Au-covered Si(111) surface to disilane at 10^{-6} Torr and 600-700ºC [2]. Oxygen exposure during growth was used to modify the nanowire growth morphology [5, 15]. Simulations use a classical

model of facet evolution [10,14] based on well-established continuum physics [16] and attachment-limited kinetics. New facets are introduced based on a linear stability analysis [10,16]. The key inputs into the model are the facet orientations and energies, the catalyst surface tension, and a parameter ε characterizing the energetics for introducing each new facet edge [10].

For silicon, the {111} facets have the lowest energy, and {001} is also stable [12]. In addition, {113} facets occur in the presence of Au [9]. Wires growing in ⟨110⟩ directions have primarily {111} sidewalls [the smooth sidewalls visible in Fig. 1(e)], along with some {001}. For wires growing in ⟨111⟩ directions, the sidewalls consist of alternating {111} and {113} facets, visible in Fig. 1(f). Thus the choice of orientation appears linked to the presence of {113} facets. We hypothesize that for the real Si system two features are essential: {111} facets have lowest energy; and there is a second set of facets, {113}, whose orientation can stabilize ⟨111⟩ growth, without eliminating geometrical frustration. To mimic this in 2D, we consider two sets of facets with 6-fold and 3-fold symmetry and respective free energies γ_6 and γ_3, as shown in Fig. 1(a,b). If $\gamma_3 \geq \gamma_6 / \cos 30°$, the equilibrium crystal shape (ECS) is hexagonal, and we consider the six equivalent facets to be analogous to Si {111}. Lower values of γ_3 introduce 3 additional facets of lower symmetry. While the new facets play a somewhat different role than the {113} facets in 3D, they meet the requirements of our hypothesis.

We begin by examining the effect of varying the facet energies in simulations. We take $\Omega_s\gamma_{vl}$=0.14 eV nm for the vapor-liquid interfacial free energy, where Ω_s and γ are respectively the atomic volume of Si and the energy per area. For the six {111}-like facets we take $\Omega_s\gamma_{vs}$=0.128 eV nm for the vapor-solid interface, and $\Omega_s\gamma_{ls}$=0.07 eV nm for the liquid-solid interface. For simplicity we take $\gamma_{3,ls}$ to be prohibitively high, so there are only {111}-like facets at the liquid-solid interface.

The key parameter controlling the behavior is then $\gamma_{3,vs}$, the energy of the new 3-fold facet at the vapor-solid interface. For $\Omega_s\gamma_{3,vs}$=0.16 eV nm as in Fig. 1(a), or for any value $\gamma_3 > \gamma_6 / \cos 30°$, we obtain the wires shown in Fig. 1(c). These are similar to prior simulations with a single set of facets having 6-fold symmetry [10], and to our experimental observations of angled wires as in Fig. 1(e). (We refer to ⟨110⟩ and ⟨112⟩ wires generically as "angled" wires.) All 9 orientations are included in all simulations; but thermodynamically unstable facets are found to never appear dynamically in the simulations.

If we lower the value of $\Omega_s\gamma_{3,vs}$, there is no change until around the value 0.148 eV nm, i.e. $\gamma_3 < \gamma_6 / \cos 30°$. Below this, we find wires growing normal to the liquid-solid interface and exhibiting sawtooth

texturing on one side, as in Fig. 1(d), with the opposite sidewall being composed of a single 3-fold facet. This asymmetry reflects the asymmetry of our crystal structure, which has no stable facet orientation on the right side of Fig. 1(b) – if it did, the wire would be smooth on both sides. The resulting wires are strikingly reminiscent of the ⟨111⟩ wires observed experimentally [2,3], as in Fig. 1(f). Strictly speaking, our model is kinetic in character with no explicit energy minimization. It is therefore all the more notable that the transition from angled to sawtooth geometry corresponds closely to the value of $\gamma_{3,vs}$ at which the sawtooth gives lower overall energy, i.e. the value where the equilibrium crystal shape develops stable extra facets.

We have verified that the size of the individual "teeth" of the sawtooth scale linearly with wire diameter, just as observed in experiment [2]. For a given wire diameter, the tooth size depends on how difficult it is to introduce the required new facets. An extra capillary force is needed because of facet-edge energetics [2], and in our model this is given by a dimensionless parameter ε as described in Ref. [10]. Here we choose ε=0.05 to give teeth that are easily visible and roughly comparable to those of Si nanowires.

Going beyond steady growth, we find that in both simulations and experiments we can reversibly switch the orientation *during growth* (Fig. 2). In simulations, we simply vary $\gamma_{3,vs}$ (or $\gamma_{6,vs}$) as above. In experiments, we introduce or discontinue a small flow of O_2. Presumably the O_2 changes the relative energies of {111} and {113} facets. Such reversible *in situ* control offers novel opportunities for device design [17]. Our simulations demonstrate why this can easily be accomplished – for frustrated growth the modes are in close competition, so only small surface energy changes are needed, conveniently accomplished during continuous growth at constant temperature by varying the vapor composition

Given the qualitatively different geometries of the two growth modes in Fig. 1, it is natural to ask how other aspects of their behavior might differ. For ⟨111⟩ growth it has been shown that Au can diffuse out of (or into) the catalyst droplet, causing nanowire tapering [15]. However, previous experimental and theoretical work on tapering has not addressed the faceted character of nanowires. We have therefore carried out simulations in both angled and sawtooth regimes, removing Au at a constant rate, and compare them with observations.

We find that sawtooth wires accommodate gradual Au loss in a continuous way, by slightly varying the ratio of the two facets comprising the sawtooth, Fig. 3(a). Experimentally, the tapering of ⟨111⟩ wires also appears continuous in this sense, Fig. 3(b). But angled wires in simulations only taper by

introducing discrete jogs, Fig. 3(c), consistent with experimental observations of smooth sides punctuated by discrete jogs, Fig. 3(d). The experimental jogs are less uniform and regular, in part because in 3D jogs occur on different sidewalls, which are not all seen in projection.

In our experiments angled wires are asymmetric, and the jogs always occur on the acute-angle side of the wire tip. The same happens in the simulations, as seen by comparing Figs. 3(c) and 3(d). Since the tapering results from coarsening of the droplets [15], some wires actually grow wider instead of narrower. The simulations predict that the resulting outward jogs should then appear on the opposite side of the wire, as shown in Fig. 3(e). While it is difficult to find widening angled wires experimentally, the example shown in Fig. 3(f) clearly corroborates the prediction. This behavior follows directly from the elementary processes by which new facets are introduced in the model [10] – for the 6-fold geometry there are no elementary processes corresponding to outward jogs at an acute edge, nor to inward jogs at an obtuse edge.

As the droplet shrinks, the same rate of Au loss gives a greater rate of diameter decrease, leading ultimately to a breakdown of wire growth. If we continue the growth from Fig. 3(a), Fig. 4(a) shows that tapering is initially accommodated by varying the relative sizes of the sawtooth facets. However, when the taper rate becomes too large, one facet ceases to occur, and the rate is fixed by the orientation of the surviving facet. When even this taper rate cannot accommodate the Au loss, other facets are introduced. The same general behavior is seen in experiment, Fig. 4(b). The set of available facets is different, so the details differ. But just as in the simulation, the breakdown of quasi-steady wire growth occurs when the sawtooth sidewall degenerates into a single facet.

An even more extreme situation occurs if we interrupt growth. As Au continues to diffuse away, the supersaturated droplet deposits Si onto the nanowire tip, just as during growth. However, because this growth is so slow compared to the rate of droplet shrinking, the taper angle becomes extreme. No known facet orientations can readily accommodate such tapering, and the experimental behavior in Fig. 4(d) appears consistent with unfacetted growth. We can understand this from the simulation in Fig. 4(c). Close examination reveals that the upper surface consists of a staircase of steps separating (111) terraces. In the simulation, the steps are tiny facets, but in the experiment they might be atomic steps. Such a staircase is the only way to satisfy the geometrical constraint as the droplet shrinks, so the supersaturation rises until it is sufficient to introduce the required steps.

It may seem surprising that a simple 2D model can reproduce so many features of the real system. The 2D hexagonal crystal already provides an adequate analogue for the dominant role of {111} facets in

angled nanowires. The most striking additional features in real 3D wires can be qualitatively understood as following simply from the stabilization of ⟨111⟩ growth without eliminating frustration. This automatically implies sawtooth faceting of the sidewalls, and all that goes with it. The stabilization of ⟨111⟩ growth in Si is accomplished by introducing new low-energy facets, specifically {113} facets. The 2D geometry of Fig. 1, though different in detail, reproduces exactly this combination of factors, introducing a new facet that stabilizes growth normal to the liquid-solid interface without eliminating geometrical frustration. The large number of experimental features reproduced by the model confirms the central role of geometrical frustration, and illustrates the power of framing simple models to test growth hypotheses.

Ge nanowires show differences from Si [6,8], and no sawtooth structure has been identified. Nevertheless, in view of the many striking similarities, we speculate that geometrical frustration plays a role in the multiple orientations known for Ge nanowires as well. Zincblende III-V semiconductor nanowires exhibit a sawtooth structure that is different from Si, involving twinning [18,19,20]. But like Si it reflects geometrical frustration [18,19], in that the only available facets are {111}. In that case there is a well-studied competition, not with a different oriention, but with a metastable crystal structure (wurtzite) that avoids geometrical frustration at the cost of higher bulk energy [19,20].

In conclusion, advances in computational modeling of nanowire VLS growth enable direct qualitative comparison between theory and *in situ* observations. We find that in Si nanowires, the absence of allowed facet orientations normal to the (111) growth interface leads to geometrical frustration. This forces the wire to adopt an unintuitive structure, and leads to a competition between very different growth modes. Small differences in growth conditions can tip the balance, explaining the coexistence of angled and sawtooth modes. There are striking qualitative differences in how these modes evolve, as illustrated here by their response to a steady change in catalyst size during coarsening. III-V semiconductor nanowires also exhibit geometrical frustration effects, and Ge may also. The unifying thread in all these system is that complex behavior is caused by the dominant role of {111} facets and the absence of facets that would allow all the sidewalls to be parallel to ⟨111⟩.

We acknowledge financial assistance from the NSF under Grant No. DMR-0907483.

* tersoff@us.ibm.com

[1] Wagner, R. S. In Whisker Technology; Levitt, A.P., Ed.; Wiley Interscience: New York, 1970; p 47.

[2] F. M. Ross, J. Tersoff, and M. C. Reuter, Phys. Rev. Lett. 95, 146104 (2005).

[3] F. Oehler et al., J., Nano Lett. 10, 2335 (2010).

[4] Y. Wu et al., Nano Lett. 4, 433 (2004).

[5] S. Kodambaka, J. B. Hannon, R. M. Tromp, and F. M. Ross, Nano Lett. 6, 1292 (2006).

[6] P. Madras, E. Dailey, J. Drucker, Nano Lett. 9, 3826 (2009).

[7] However, liquid-solid interfaces normal to the ⟨110⟩ or ⟨112⟩ growth axis are reported in Ref. [6], perhaps due to different growth conditions.

[8] E. Dailey, P. Madras, J. Drucker, Appl. Phys. Lett. 97, 143106 (2010).

[9] C. Wiethoff et al., Nano Lett. 8, 3065 (2008).

[10] K. W. Schwarz and J. Tersoff, Nano Lett. 11, 316 (2011).

[11] V. Schmidt, S. Senz, and U. Gösele, Nano Lett. 5, 931-935 (2005).

[12] D. J. Eaglesham et al., Phys. Rev. Lett. 70, 1643–1646 (1993).

[13] For ⟨111⟩ wires, the sidewalls are often said to be {112} facets [1]. However, in reality {112} facets are unstable in this system [9], and the sidewalls are actually composed of nanoscale {111} and {113} facets [2,3].

[14] K. W. Schwarz and J. Tersoff, Phys. Rev. Lett. 102, 206101 (2009).

[15] J. B. Hannon, S. Kodambaka, F. M. Ross, and R. M. Tromp, Nature 440, 69 (2006).

[16] Carter, W. C.; Roosen, A. R.; Cahn, J. W.; Taylor, J. E. Acta Metall. Mater. 43, 4309 (1995).

[17] B. Tian et al., Nature Nanotech. 4, 824 (2009).

[18] L. S. Karlsson et al., Nanotech. 18, 485717 (2007).

[19] R. E. Algra et al., Nature 456, 369–372 (2008).

[20] P. Caroff et al,, Nature Nanotech. 4, 50–55 (2008).

Figure captions

Figure 1. (a, b) Wulff construction of the 2D equilibrium crystal shapes used in simulations. (a) $\gamma_{3,vs}=1.25\times\gamma_{6,vs}$; 6 thermodynamically stable facet orientations are available, (b) $\gamma_{3,vs}=1.15\times\gamma_{6,vs}$; 9 stable facets. (c) Simulation with $\gamma_{3,vs}$ as in (a), giving angled wires. (d) Simulation with $\gamma_{3,vs}$ as in (b), giving sawtooth wires. (e) 47nm-diameter Si nanowire imaged during growth at 645ºC and 1.2×10^{-6} Torr disilane + 1×10^{-7} Torr oxygen. (f) 220 nm-diameter Si nanowire imaged during growth at 600ºC and 2×10^{-6} Torr disilane, adapted from [2]. The sawtooth structure is not well resolved on the left sidewall, giving a misleading impression that it is smooth as in (d). Both nanowires are viewed in the $[1\bar{1}0]$ direction.

Figure 2.

(a) Reversible switching using O_2 of a 30nm diameter Si nanowire imaged at 700ºC and 2×10^{-6} Torr disilane with 2×10^{-7} Torr oxygen added at the times indicated (in minutes; arbitrary zero). Growth changes direction by ~33º, consistent with switching between ⟨110⟩ and ⟨111⟩ directions. The small features on the sidewall are polycrystalline Si that grows on the oxidized surfaces of the wire. (b) Simulation of reversible switching by changing $\gamma_{3,vs}$ between the two values used in Fig. 1.

Figure 3. (a) Simulation of ⟨111⟩-like wire [as in Fig. 1(d)], but with gradual Au loss. (b) Si nanowire imaged after growth at 575ºC and 1×10^{-6} Torr disilane. (c) Simulation of angled wire [as in Fig. 1(c)], with gradual Au loss. Arrows indicate the discrete jogs. (d) Si nanowire imaged during growth at 575ºC and 1×10^{-6} Torr disilane + 1×10^{-7} Torr oxygen. (e) Simulation of angled wire with gradual Au gain. Arrows indicate the discrete jogs. (f) Si nanowire imaged during growth under the same conditions as (d). The dark bands are extended defects consistent with multiple twinning.

Figure 4.

(a,b) Final shape of a ⟨111⟩ wire whose catalyst has shrunk away due to Au diffusion during growth. Growth conditions in simulation (a) and experiment (b) are as in Fig. 3(a) and 3(b) respectively. Arrows highlight last three "sawteeth" before the extended {111} facet. (c,d) Final shape of a ⟨111⟩ wire in simulation (c) and experiment (d), where growth was stopped without changing temperature, so Au continued to diffuse away. In (c), the top surface appears smooth but is composed of tiny facets from the allowed set.

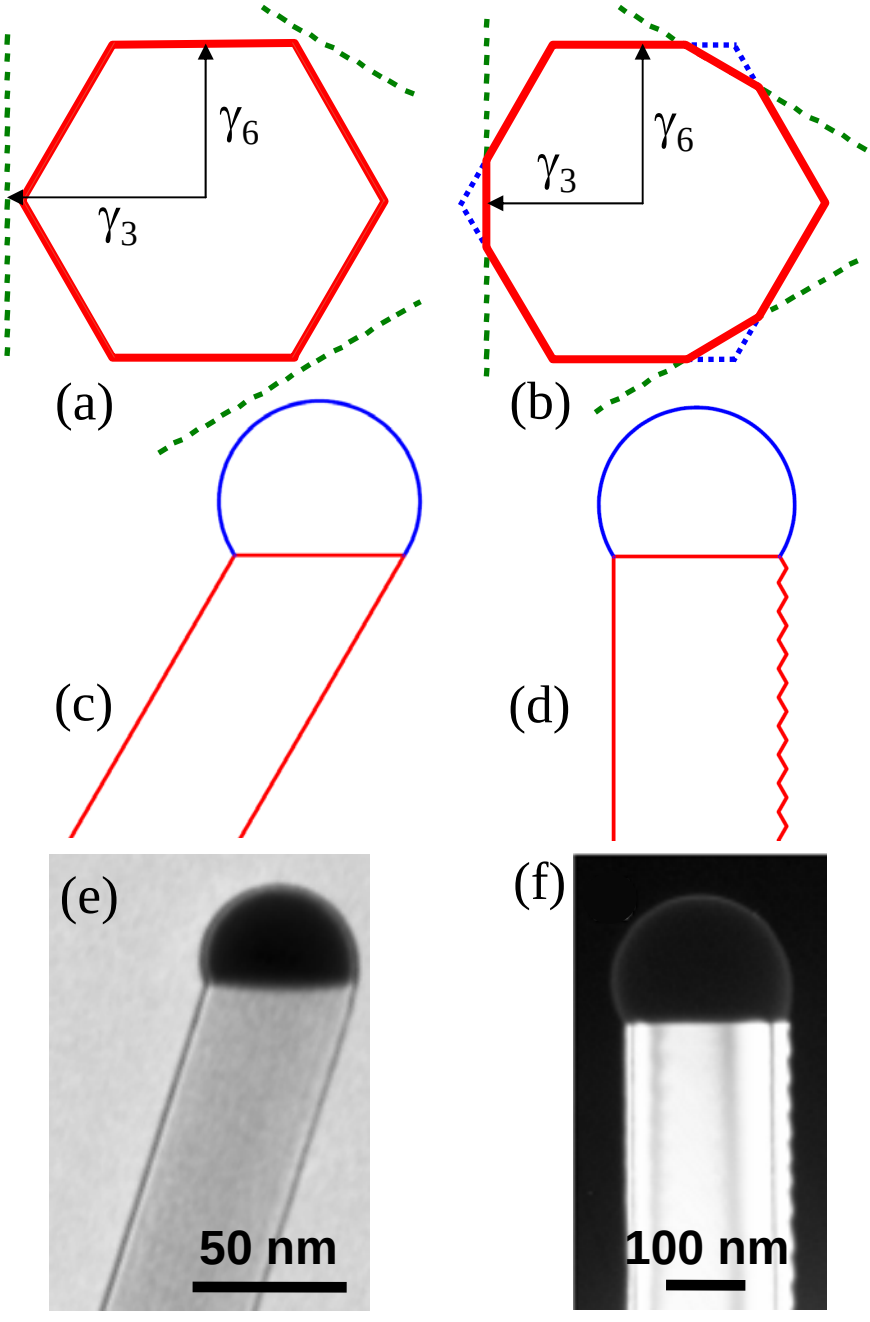
γ_6
γ_3
(a)
γ_3
γ_6
(b)
(c)
(d)
(e)
50 nm
(f)
100 nm

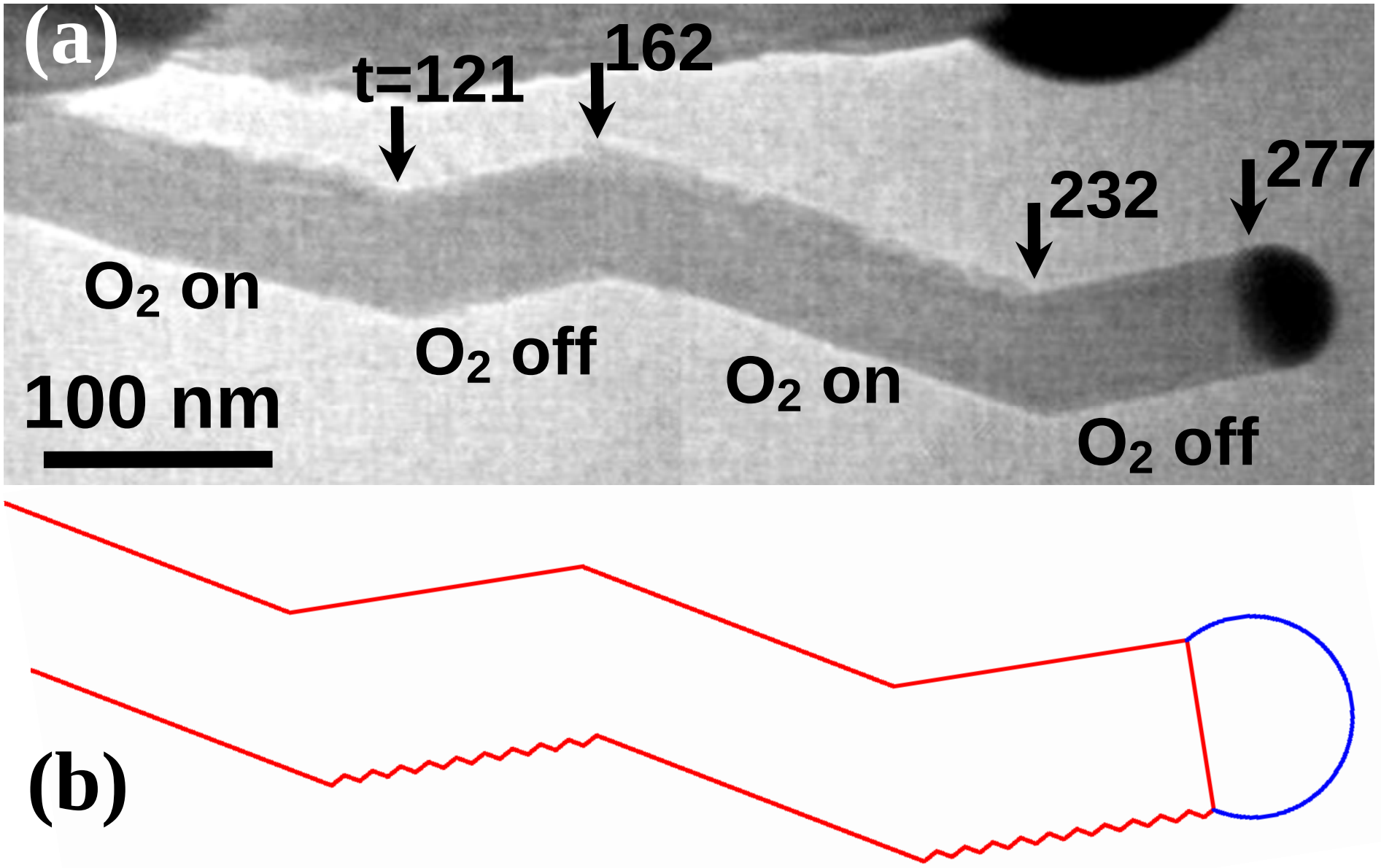
(a)
t=121
162
232
277
O2 on
O2 off
O2 on
O2 off
100 nm
(b)

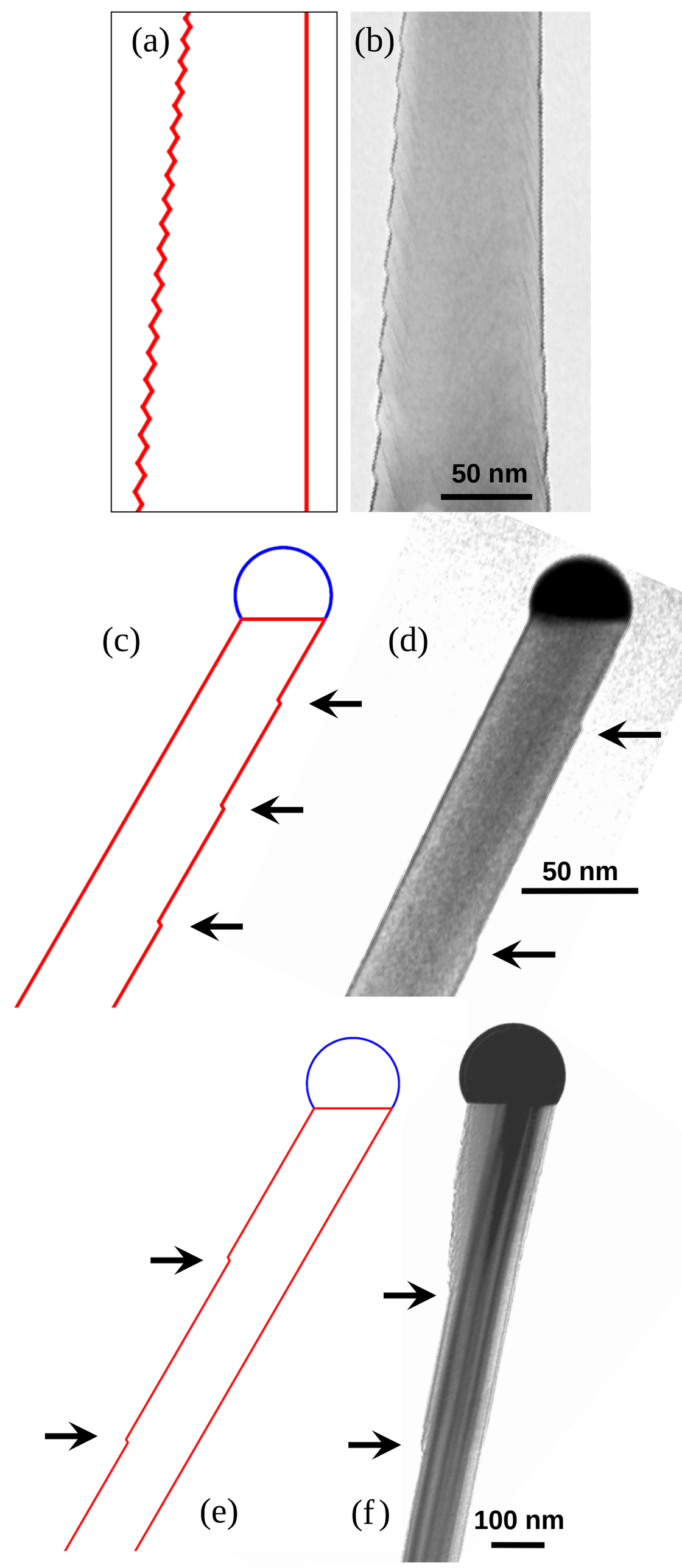
(a)
(b)
50 nm
(c)
(d)
50 nm
(e)
(f)
100 nm

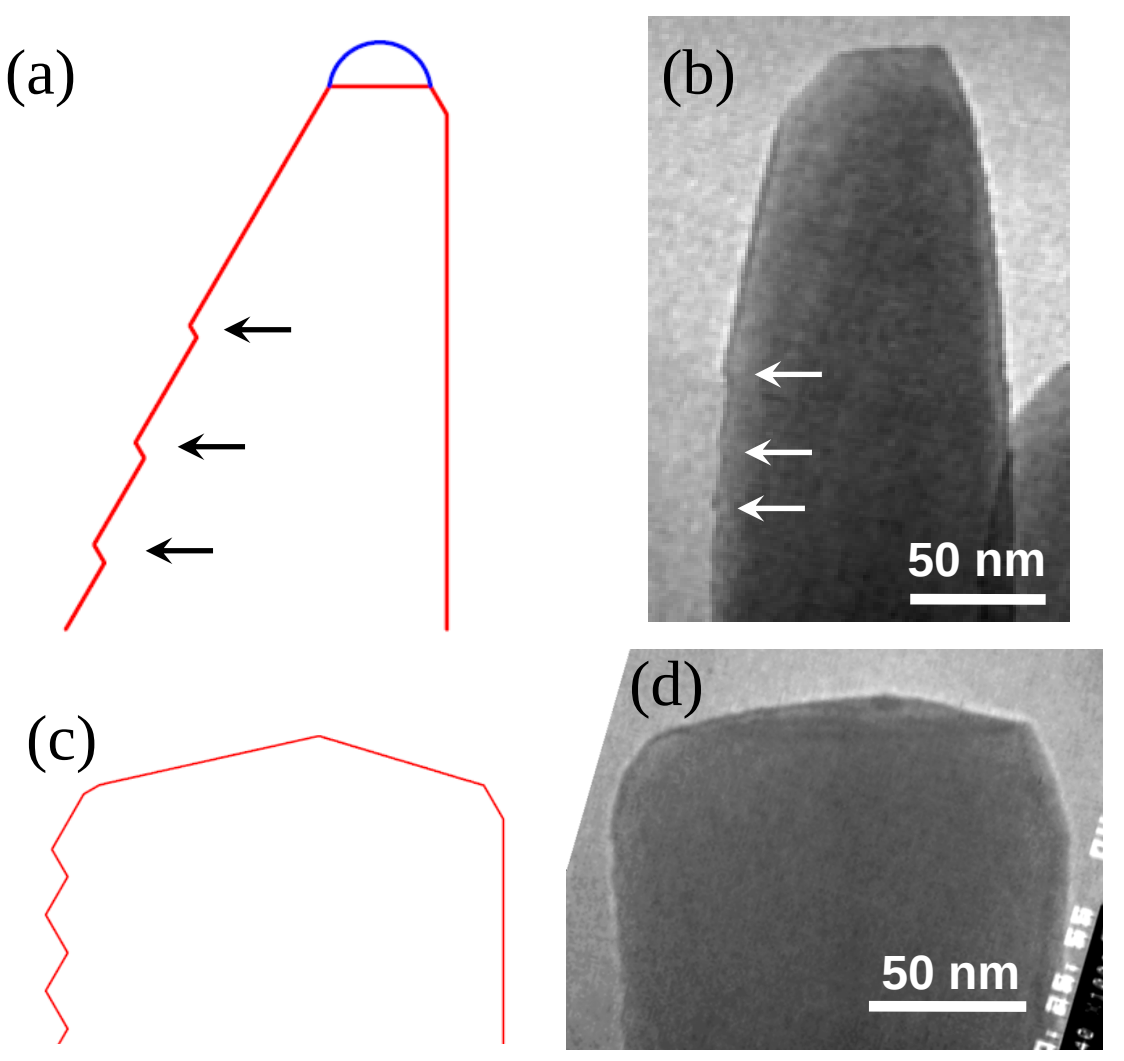
(a)
(b)
50 nm
(c)
(d)
50 nm